

Anisotropy of the upper critical field in a heavy-fermion superconductor

C. H. Choi

Department of Physics, Kyungwon University, Sunghnam-shi, Kyunggi-do 461-701, Korea

J. A. Sauls

Department of Physics and Astronomy, Northwestern University, Evanston, Illinois 60208

(Received 15 July 1993)

We study the upper critical field for various possible order parameters of a heavy-fermion superconductor. We pay particular attention to the question of how the anisotropy of the upper critical field changes by effects of paramagnetism, impurity scattering, and Fermi-surface anisotropy in the presence of strong spin-orbit coupling. The paramagnetic limit can have a dramatic effect on the anisotropy in odd-parity superconductors, and provide important information on the symmetry of underlying order parameters. We also discuss the effect of impurity scattering.

I. INTRODUCTION

The upper critical field H_{c2} of heavy-fermion superconductors shows many interesting features.¹ Single-crystal UPt₃ has an unusual temperature dependence at low temperature, as well as a kink structure near the transition temperature.²⁻⁴ For $U_{1-x}\text{Th}_x\text{Be}_{13}$ the upper critical field rises steeply in the Ginzburg-Landau region and deviates quite early from its linear slope.⁵ Choi and Sauls (referred to as CS) have previously presented a theoretical explanation for the unusual temperature-dependence of H_{c2} for UPt₃ and discussed how the paramagnetic effect can provide crucial information on the spin-structure of underlying order parameters in heavy-fermion superconductors.⁶ In this paper we present detailed calculations of the upper critical field for heavy-fermion superconductors whose crystal symmetry belongs to the hexagonal point group D_{6h} , which includes UPt₃, UNi₂Al₃ and UPd₂Al₃.^{7,8} We compute the upper critical field for all temperature, while taking into account key elements to determine the anisotropy of H_{c2} in heavy-fermion superconductors; anisotropy of order parameters, Fermi-surface anisotropy, paramagnetic effect, impurity scattering as well as the strong spin-orbit coupling.

The anisotropy of H_{c2} of pure superconductor is determined by the anisotropy of the Fermi surface near the transition temperature, where the paramagnetic coupling is unimportant. At lower temperatures, however, the paramagnetic limit can have a dramatic effect on the an-

isotropy of H_{c2} in odd-parity superconductors. For even-parity states, the upper critical field is bounded by the paramagnetic effect for all directions of field. But for odd-parity states, there is no suppression of superconductivity if the external field is along the direction of Cooper-pair spin, whereas the magnetic field of other orientations will be a pair-breaking source.⁹ We also study the effect of impurity scattering on H_{c2} . Nonmagnetic impurities can be pair breaking even in the absence of applied field for the unconventional superconductors whose order parameters belong to the nonidentity representations.¹⁰ This leads to a change in the slope of H_{c2} near the transition temperature and the anisotropy of H_{c2} .

In Sec. II we derive general equations for the upper critical field, while incorporating an arbitrary Fermi surface, paramagnetic effect, Fermi-liquid corrections, impurity scattering, and the unconventional order parameters. In Sec. III we discuss the effect of paramagnetism on the anisotropy of H_{c2} in clean limit. The effect of impurity scattering is considered in Sec. IV.

II. FORMALISM

We use the quasiclassical theory of superconductivity and follow closely the notation of CS and Alexander *et al.*¹¹ The key quantity to compute is the quasiclassical propagator $\hat{g}(\mathbf{k}_f, \mathbf{R}, \epsilon)$, which is a 4×4 matrix in the Nambu representation:

$$\hat{g} = \begin{pmatrix} g(\mathbf{k}_f, \mathbf{R}, \epsilon) + \mathbf{g}(\mathbf{k}_f, \mathbf{R}, \epsilon) \cdot \boldsymbol{\sigma} & [f(\mathbf{k}_f, \mathbf{R}, \epsilon) + \mathbf{f}(\mathbf{k}_f, \mathbf{R}, \epsilon) \cdot \boldsymbol{\sigma}] i \sigma_y \\ i \sigma_y [f^*(-\mathbf{k}_f, \mathbf{R}, \epsilon) - \mathbf{f}^*(-\mathbf{k}_f, \mathbf{R}, \epsilon) \cdot \boldsymbol{\sigma}] & g^*(-\mathbf{k}_f, \mathbf{R}, \epsilon) - \sigma_y \mathbf{g}^*(-\mathbf{k}_f, \mathbf{R}, \epsilon) \cdot \boldsymbol{\sigma} \sigma_y \end{pmatrix}, \quad (1)$$

where $\boldsymbol{\sigma} = (\sigma_x, \sigma_y, \sigma_z)$, are the Pauli matrices in spin space. Here ϵ is the Matsubara frequency, \mathbf{R} is the real-space position, and \mathbf{k}_f is a two-dimensional coordinate defining the position on the Fermi surface. The quasiclassical propagator satisfies a transportlike equation:

$$[i\epsilon \hat{\tau}_3 - \hat{\sigma}_{\text{self}}(\mathbf{k}_f, \mathbf{R}, \epsilon) - \hat{\nu}_{\text{ext}}(\mathbf{k}_f, \mathbf{R}), \hat{g}(\mathbf{k}_f, \mathbf{R}, \epsilon)] + i \mathbf{v}_f(\mathbf{k}_f) \cdot \nabla_{\mathbf{R}} \hat{g}(\mathbf{k}_f, \mathbf{R}, \epsilon) = 0, \quad (2)$$

$$\hat{g}^2 = -\pi^2. \quad (3)$$

The Fermi velocity $\mathbf{v}_f(\mathbf{k}_f)$ depends on \mathbf{k}_f and $\hat{\tau}_3$ is a Pauli matrix in particle-hole space. The coupling to a magnetic field is given by

$$\hat{v}_{\text{ext}}(\mathbf{k}_f, \mathbf{R}) = \frac{e}{c} \mathbf{v}_f(\mathbf{k}_f) \cdot \mathbf{A}(\mathbf{R}) \hat{\tau}_3 + \mu(\mathbf{k}_f) \hat{\mathbf{S}} \cdot \mathbf{B}(\mathbf{R}). \quad (4)$$

The first term is the orbital coupling to the field, while the second term is the paramagnetic coupling to the spin. Here e and $\mu(\mathbf{k}_f)$ are electric charge and effective magnetic moment of a quasiparticle and c is speed of light. The vector potential $\mathbf{A}(\mathbf{R})$ generates the total field $\mathbf{B} = \nabla \times \mathbf{A}$ and $\hat{\mathbf{S}}$ is the spin operator:

$$\hat{\mathbf{S}} = \begin{bmatrix} \sigma & 0 \\ 0 & -\sigma_y \sigma \sigma_y \end{bmatrix}. \quad (5)$$

The self-energy $\hat{\sigma}_{\text{self}}$ includes the pairing self-energy $\hat{\Delta}(\mathbf{k}_f, \mathbf{R})$ as well as the self-energies for impurity scattering and Fermi-liquid corrections. One simplifying feature is that we need the propagator \hat{g} only to the first order in $\hat{\Delta}$ in order to compute the upper critical field so that the diagonal component of \hat{g} can be replaced by the

normal-state propagator. The Fermi-liquid corrections can then be absorbed in the definition of effective magnetic moment $\mu(\mathbf{k}_f)$. The equation for impurity self-energy can be written

$$\hat{\sigma}_{\text{imp}}(\mathbf{k}_f, \mathbf{R}, \epsilon) = \langle w(\mathbf{k}_f, \mathbf{k}'_f) \hat{g}(\mathbf{k}'_f, \mathbf{R}, \epsilon) \rangle_{\mathbf{k}'_f}, \quad (6)$$

where the bracket $\langle \dots \rangle_{\mathbf{k}'_f}$ denotes a Fermi surface integration over the variable \mathbf{k}'_f and $w(\mathbf{k}_f, \mathbf{k}'_f)$ is a scattering probability of nonmagnetic impurities. Note that Eq. (6) is valid beyond the Born approximation in our calculation.¹²

By solving the off-diagonal component of \hat{g} from Eqs. (2) and (3) together with the self-consistent equation for impurity self-energy and the weak-coupling gap equation, we obtain the following coupled equations. For odd-parity states,

$$\Delta(\mathbf{k}_f, \mathbf{R}) = T \sum_{\epsilon} \langle V^{\text{odd}}(\mathbf{k}_f, \mathbf{k}'_f) \mathbf{f}(\mathbf{k}'_f, \mathbf{R}, \epsilon) \rangle_{\mathbf{k}'_f}, \quad (7)$$

where

$$\begin{aligned} \mathbf{f}(\mathbf{k}_f, \mathbf{R}, \epsilon) = & 2\pi \int_0^{\infty} d\tau \exp(-\tau \hat{L}) \{ [1 + \{\cos(2\tau\mu H) - 1\} \hat{h} \hat{h}^{\text{tr}}] [\Delta(\mathbf{k}_f, \mathbf{R}) + \langle w(\mathbf{k}_f, \mathbf{k}'_f) \mathbf{f}(\mathbf{k}'_f, \mathbf{R}, \epsilon) \rangle_{\mathbf{k}'_f}] \\ & - i \text{sgn}(\epsilon) \sin(2\tau\mu H) \hat{h} \langle w(\mathbf{k}_f, \mathbf{k}'_f) \mathbf{f}(\mathbf{k}'_f, \mathbf{R}, \epsilon) \rangle_{\mathbf{k}'_f} \}, \end{aligned} \quad (8)$$

$$\begin{aligned} f(\mathbf{k}_f, \mathbf{R}, \epsilon) = & 2\pi \int_0^{\infty} d\tau \exp(-\tau \hat{L}) \{ \cos(2\tau\mu H) \langle w(\mathbf{k}_f, \mathbf{k}'_f) \mathbf{f}(\mathbf{k}'_f, \mathbf{R}, \epsilon) \rangle_{\mathbf{k}'_f} - i \text{sgn}(\epsilon) \sin(2\tau\mu H) \hat{h}^{\text{tr}} \\ & \times [\Delta(\mathbf{k}_f, \mathbf{R}) + \langle w(\mathbf{k}_f, \mathbf{k}'_f) \mathbf{f}(\mathbf{k}'_f, \mathbf{R}, \epsilon) \rangle_{\mathbf{k}'_f}] \}. \end{aligned} \quad (9)$$

The operator \hat{L} is defined by

$$\hat{L} = 2|\epsilon| + 2\pi w_0 + \text{sgn}(\epsilon) \mathbf{v}_f \cdot \partial, \quad (10)$$

where $\partial = \nabla_{\mathbf{R}} + i(2e/c) \mathbf{A}$ and w_0 is an s -wave part of $w(\mathbf{k}_f, \mathbf{k}'_f)$. The pairing interaction is denoted by $V^{\text{odd}}(\mathbf{k}_f, \mathbf{k}'_f)$, the direction of magnetic field by the unit vector \hat{h} , and its transpose by $\hat{h}^{\text{tr}} = (h_x, h_y, h_z)$. Note that singlet and triplet components of the propagator, f and \mathbf{f} , decouple without the paramagnetic terms. The equations for even-parity states can be obtained from Eqs. (7)–(9) with the following substitutions:

$$\mathbf{f} \leftrightarrow f, \quad \Delta \leftrightarrow \Delta, \quad \hat{h} \leftrightarrow \hat{h}^{\text{tr}}, \quad V^{\text{odd}} \leftrightarrow V^{\text{even}}. \quad (11)$$

The upper critical field is then computed as the largest value of H for which Eq. (7) has a nontrivial solution.

In a pure superconductor the equations are greatly simplified. For odd-parity,

$$\Delta(\mathbf{k}_f, \mathbf{R}) = 2\pi T \sum_{\epsilon} \int_0^{\infty} d\tau \langle V^{\text{odd}}(\mathbf{k}_f, \mathbf{k}'_f) \exp\{-2\tau|\epsilon| - \text{sgn}(\epsilon) \tau \mathbf{v}_f(\mathbf{k}'_f) \cdot \partial\} [1 + \{\cos(2\tau\mu H) - 1\} \hat{h} \hat{h}^{\text{tr}}] \Delta(\mathbf{k}'_f, \mathbf{R}) \rangle_{\mathbf{k}'_f}. \quad (12)$$

For even-parity, the scalar order parameter satisfies the similar equation to Eq. (12) with a substitution, $\hat{h} \hat{h}^{\text{tr}} \rightarrow 1$. Note that the paramagnetic term is unimportant near the transition temperature for both odd- and even-parity states; however, it can have a large effect on H_{c2} at low temperatures, except for the case of odd-parity states with $\Delta \perp \mathbf{H}$.

For numerical calculations we use the same material parameters as in CS with an extension to take into account impurity scattering: (i) two Fermi velocities, v_f^{\parallel} and v_f^{\perp} , to parametrize our uniaxial model for the Fermi surface, (ii) an isotropic effective magnetic moment μ (Ref. 13), (iii) an isotropic part of impurity scattering w_0 ,

and (iv) superconducting transition temperatures, T_c and T_{c0} , with and without impurities (in zero field), respectively. We also introduce the coherence lengths, $\xi_{\perp} = v_f^{\perp} / 2\pi T_{c0}$, $\xi_{\parallel} = v_f^{\parallel} / 2\pi T_{c0}$, and a magnetic scale, $H_0 = (hc/2e) / \pi \xi_{\perp}^2$, as well as the dimensionless parameters.

$$\begin{aligned} \eta = & \left[\frac{\xi_{\parallel}}{\xi_{\perp}} \right]^2, \quad \bar{\mu} = \frac{\mu H_0}{\pi T_{c0}}, \quad \bar{w}_0 = \frac{w_0}{T_{c0}}, \\ t_c = & \frac{T_c}{T_{c0}}, \quad t = \frac{T}{T_{c0}}, \quad h = \frac{H}{H_0}. \end{aligned} \quad (13)$$

The upper critical field is calculated with \mathbf{H} along \hat{z} , the axis of sixfold symmetry, and also for \mathbf{H} in the basal plane.

III. PARAMAGNETIC EFFECT

We compute the upper critical field in the clean limit. First we consider the odd-parity state; the two-dimensional (2D) representations, E_{1u} and E_{2u} , and also the B_{1u} representation, which for our purpose is representative of all the 1D odd-parity states.⁷ For the E_{1u} state the pairing potential and order parameter are:

$$V^{\text{odd}}(\mathbf{k}_f, \mathbf{k}'_f) = \lambda \hat{z} \hat{z}^{\text{tr}} [\psi^*(\mathbf{k}_f) \psi(\mathbf{k}'_f) + \psi(\mathbf{k}_f) \psi^*(\mathbf{k}'_f)], \quad (14)$$

$$\Delta(\mathbf{k}_f, \mathbf{R}) = \hat{z} [\eta_+(\mathbf{R}) \psi^*(\mathbf{k}_f) + \eta_-(\mathbf{R}) \psi(\mathbf{k}_f)], \quad (15)$$

where λ is a coupling constant and $\psi(\mathbf{k}_f) \sim k_x + ik_y$. Note that Δ is along \hat{z} , so that the Cooper pair spin lies in the basal plane. By putting Eqs. (14) and (15) into the gap equation (12), we obtain equations for the amplitudes $\eta_{\pm}(\mathbf{R})$:

$$\begin{bmatrix} \eta_+ \\ \eta_- \end{bmatrix} = \begin{bmatrix} K_{\text{on}} & K_{\text{off}} \\ K_{\text{off}}^* & K_{\text{on}} \end{bmatrix} \begin{bmatrix} \eta_+ \\ \eta_- \end{bmatrix}, \quad (16)$$

where

$$\alpha_n = \lambda 4\pi T \sum_{\epsilon \geq 0} \int_0^{\infty} d\tau \langle |\psi|^2 \exp \left[-2\tau\epsilon - \frac{1}{2}p^2 \right] \cos(2\tau\mu H) L_n^0(p^2) \rangle, \quad (21)$$

$$\beta_n = \lambda 4\pi T \sum_{\epsilon \geq 0} \int_0^{\infty} d\tau \langle |\psi|^2 \exp \left[-2\tau\epsilon - \frac{1}{2}p^2 \right] \cos(2\tau\mu H) \frac{p^2 L_n^2(p^2)}{\sqrt{(n+1)(n+2)}} \rangle, \quad (22)$$

where $p^2 = eH(\tau v_f^1)^2/c$, and L_n^k is a generalized Laguerre polynomial. Here we have used the formula

$$\exp(-\tau \mathbf{v}_f \cdot \partial) \phi_n(\mathbf{R}) = \sum_{m=0}^n \sum_{l=0}^{\infty} \exp \left\{ -\frac{p^2}{2} + i\theta(m-l) \right\} p^{m+l} \frac{(-1)^m}{m!l!} \frac{\sqrt{n!(n-m+l)!}}{(n-m)!} \phi_{n-m+l}(\mathbf{R}), \quad (23)$$

where θ is an angle variable of the Fermi velocity, \mathbf{v}_f^1 , in basal plane.

The maximum value of H_{c2} occurs for $(\eta_+, \eta_-) \sim (\phi_2, c_0 \phi_0)$ with $c_0 = \beta_0/(1-\alpha_0)$, that is,¹⁵

$$\Delta(\mathbf{k}_f, \mathbf{R}) \sim \hat{z} [\phi_2(\mathbf{R})(k_x - ik_y) + c_0 \phi_0(\mathbf{R})(k_x + ik_y)]. \quad (24)$$

The limiting values of H_{c2} at $T=0$ and close to T_{c0} are listed in the Table I of CS.

When the magnetic field lies in the basal plane, the upper critical field is independent of paramagnetism because the Cooper pairs have no amplitude with zero spin projection for directions in the plane. As a consequence of uniaxial symmetry of the Fermi surface H_{c2} is isotropic in the basal plane at all temperatures, and we can choose a direction of magnetic field along the \hat{x} axis. It is then convenient to work in a basis of (η_1, η_2) in which equations for η_1 and η_2 decouple. Here $\eta_1 = (\eta_+ + \eta_-)/\sqrt{2}$ and $\eta_2 = -i(\eta_+ - \eta_-)/\sqrt{2}$. The equation for η_1 becomes

$$K_{\text{on}} = \lambda 4\pi T \sum_{\epsilon \geq 0} \int_0^{\infty} d\tau \langle |\psi|^2 \exp(-2\tau\epsilon - \tau \mathbf{v}_f \cdot \partial) \times [1 + \{\cos(2\tau\mu H) - 1\} \cos^2(\theta_h)] \rangle. \quad (17)$$

The angle between magnetic field \hat{h} and the \hat{z} axis of the crystal is denoted by θ_h . The matrix element K_{off} has the same expression as K_{on} except that $|\psi|^2$ is replaced by ψ^2 . We solve Eq. (16) for all temperature by a standard method of introducing raising and lowering operators, \hat{a}_{\pm} , and a set of eigenfunctions, $\{\phi_n(\mathbf{R})\}$, of the harmonic oscillator problem.¹⁴

When the magnetic field is along \hat{z} , we define $\hat{a}_+ = -\frac{1}{2}(\partial_x + i\partial_y)$ and $\hat{a}_- = \frac{1}{2}(\partial_x - i\partial_y)$, and then expand $\eta_{\pm}(\mathbf{R})$ in terms of $\{\phi_n(\mathbf{R})\}$:

$$\eta_{\pm}(\mathbf{R}) = \sum_{n=0}^{\infty} P_n^{\pm} \phi_n(\mathbf{R}). \quad (18)$$

Putting Eq. (18) into Eq. (16) yields a matrix equation for P_n^{\pm} . This can be diagonalized in a block form and its eigenvalues are obtained from the equations

$$\alpha_0 = 1, \quad (19)$$

$$(1-\alpha_n)(1-\alpha_{n+2}) = \beta_n^2, \quad \text{for } n \geq 0, \quad (20)$$

where

$$\lambda 4\pi T \sum_{\epsilon \geq 0} \int_0^{\infty} d\tau \langle \psi_1^2 \exp(-2\tau\epsilon - \tau \mathbf{v}_f \cdot \partial) \rangle \times \eta_1(\mathbf{R}) = \eta_1(\mathbf{R}), \quad (25)$$

where $\psi_1 \sim k_x$. A similar equation holds for η_2 with $\psi_2 \sim k_y$. We solve Eq. (25) by a variational method, i.e., by introducing a parameter α in the operators of harmonic oscillator,

$$\hat{a}_{\pm} = \pm \frac{1}{2}(\partial_z \mp i\alpha \partial_y), \quad (26)$$

and their corresponding eigenfunctions $\{\phi_n(\mathbf{R}, \alpha)\}$.

The maximum H_{c2} occurs when $\eta_1 = \phi_0(\mathbf{R}, \alpha)$ with $\alpha = 1/\sqrt{\eta}$, which corresponds to a rescaling of the Fermi surface and diagonalizes Eq. (25) exactly. As a remark we note that the eigenvalue equation for η_2 cannot be solved exactly by a simple rescaling of the Fermi surface because the exact eigenfunction is a linear combination of all ϕ_{2n} 's with $n \geq 0$. However, it turns out that a simple

trial function, $\eta_2 = \phi_0(\mathbf{R}, \alpha)$ with an optimum value of α , provides a good estimate for H_{c2} . Addition of other terms such as ϕ_2 and ϕ_4 in the trial function does not increase the value of H_{c2} by more than 1%.

In Fig. 1 we summarize the results for E_{1u} representation for several choices of the effective mass ratio η and scaled effective moment $\bar{\mu}$. Both h_{c2}^{\parallel} and h_{c2}^{\perp} are scaled in units of H_0 , in which h_{c2}^{\parallel} is independent of η , while h_{c2}^{\perp} scales as $1/\sqrt{\eta}$. As noted earlier the paramagnetic effect can significantly reduce the value of h_{c2}^{\parallel} at low temperatures, whereas it has no effect on h_{c2}^{\perp} . Thus, by adjusting the values of η and $\bar{\mu}$, we can *easily* make the upper critical fields h_{c2}^{\parallel} and h_{c2}^{\perp} cross over each other at finite temperature and fit the experimental data quite well.⁶

For the E_{2u} representation the order parameter

$$\Delta(\mathbf{k}_f, \mathbf{R}) = \frac{\hat{x} + i\hat{y}}{\sqrt{2}} \eta_+(\mathbf{R}) \psi(\mathbf{k}_f) - \frac{\hat{x} - i\hat{y}}{\sqrt{2}} \eta_-(\mathbf{R}) \psi^*(\mathbf{k}_f), \quad (27)$$

with $\psi(\mathbf{k}_f) \sim k_x + ik_y$, differs significantly in its spin structure from that of E_{1u} . Close to T_{c0} we have

$$h_{c2} = \frac{5}{7\xi(3)} \left[\cos^2 \theta_h + \frac{\eta}{2} \sin^2 \theta_h \right]^{-1/2} (1-t), \quad (28)$$

for an arbitrary direction of the field. Here $\xi(3)$ is the Riemann zeta function. When $\mathbf{H} \parallel \hat{z}$, following the similar steps as in the E_{1u} representation, we find that the upper

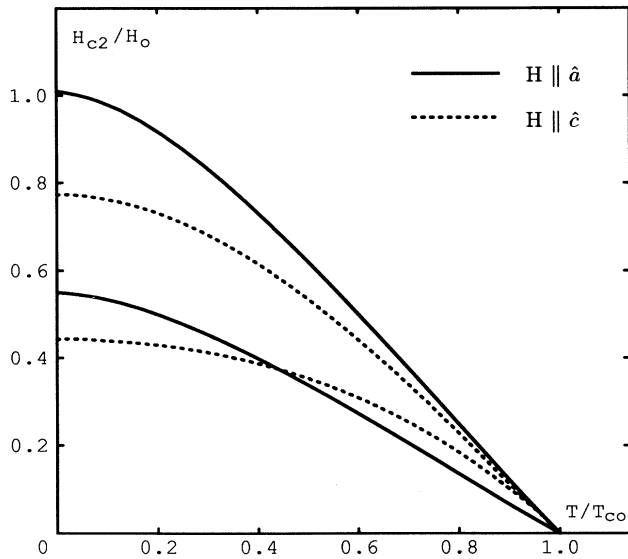


FIG. 1. Plot of $H_{c2}^{\parallel}(\mathbf{H} \parallel \hat{c})$ and $H_{c2}^{\perp}(\mathbf{H} \parallel \hat{a})$ vs T for the E_{1u} representation in the clean limit. The top two curves are for H_{c2}^{\parallel} and H_{c2}^{\perp} for an isotropic Fermi surface ($\eta=1$) and without the paramagnetic coupling ($\bar{\mu}=0$), while the bottom two are for $\eta=3.37$ and $\bar{\mu}=0.68$. Note that H_{c2}^{\parallel} is suppressed by the paramagnetic coupling at low temperature, while H_{c2}^{\perp} is independent of $\bar{\mu}$. We can easily make H_{c2}^{\parallel} and H_{c2}^{\perp} cross over with a suitable choice of parameters, as shown in the bottom two curves.

critical field is independent of the paramagnetic term and has a maximum eigenvalue for $(\eta_+, \eta_-) \sim (\phi_0, 0)$. For fields in the basal plane, H_{c2} is sensitive to $\bar{\mu}$ and we use a trial function of the form $(\eta_1, \eta_2) \sim (\phi_0, 0)$ for a variational calculation. We summarize the results in Fig. 2. We can obtain a weak crossover of the upper critical fields even without the paramagnetic term for a limited range of η , $2 < \eta < 3$; however, an important point is that H_{c2} becomes more isotropic as $\bar{\mu}$ increases.

There are four odd-parity, 1D representations in the limit of strong spin-orbit coupling, all of which have a similar spin structure to that of the E_{1u} representation, and therefore exhibit similar anisotropic paramagnetic effects. For the B_{1u} representation $\Delta(\mathbf{k}_f, \mathbf{R}) = \hat{z} \eta(\mathbf{R}) \psi(\mathbf{k}_f)$ with $\psi \sim k_x^3 - 3k_x k_y^2$. Close to T_{c0} we obtain

$$h_{c2} = \frac{9}{14\xi(3)} \left[\cos^2 \theta_h + \frac{\eta}{4} \sin^2 \theta_h \right]^{-1/2} (1-t). \quad (29)$$

Away from T_{c0} we use a trial function ϕ_0 to calculate H_{c2} for both principal directions of the field; H_{c2} depends on $\bar{\mu}$ only for $\mathbf{H} \parallel \hat{z}$. A numerical calculation shows that we can make the anisotropy ratio of upper critical fields, $h_{c2}^{\parallel}/h_{c2}^{\perp}$, almost identical to that of E_{1u} by a suitable choice of parameters, η and $\bar{\mu}$.⁶

The most important distinction of even-parity states is that the paramagnetic term is important for any direction of the magnetic field. For the E_{2g} representation,

$$\Delta(\mathbf{k}_f, \mathbf{R}) = \eta_+(\mathbf{R}) \psi(\mathbf{k}_f) + \eta_-(\mathbf{R}) \psi^*(\mathbf{k}_f), \quad (30)$$

where $\psi(\mathbf{k}_f) \sim (k_x + ik_y)^2$. When $\mathbf{H} \parallel \hat{z}$ the upper critical field can be computed exactly with $(\eta_+, \eta_-) \sim (\phi_4, c'_0 \phi_0)$ with a constant c'_0 . For $\mathbf{H} \parallel \hat{x}$ we perform a variational

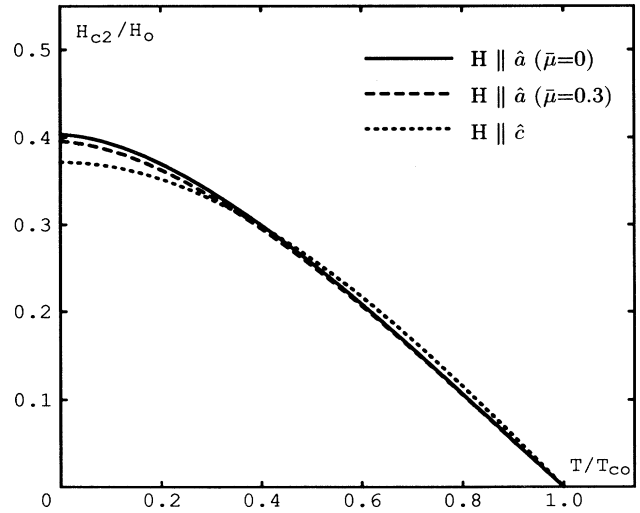


FIG. 2. Similar plot as in Fig. 1 for the E_{2u} representation. H_{c2}^{\parallel} is independent of the paramagnetic effect. The anisotropy ratio, $\eta=2.6$, is chosen to show a crossover at finite temperature. Note that the paramagnetic coupling makes the upper critical field more isotropic.

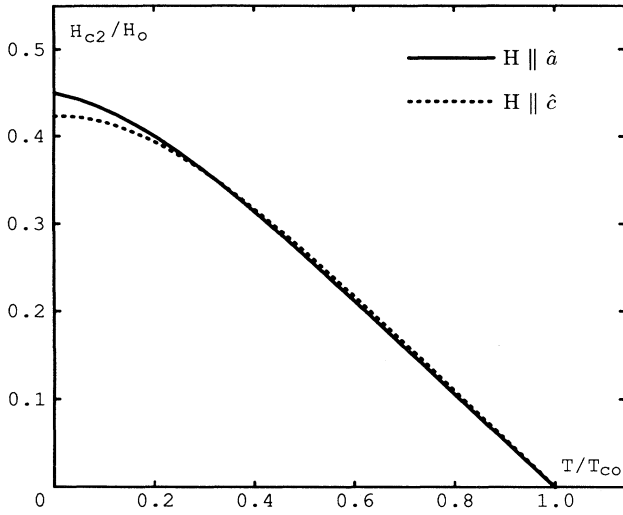


FIG. 3. Similar plot as in Fig. 1 for the E_{2g} representation. We choose $\eta=3.7$ and $\bar{\mu}=0$, where a very weak crossover is possible. For a nonzero value of $\bar{\mu}$ the upper critical field becomes even more isotropic. For even-parity representations H_{c2} is bounded by the paramagnetic limit for any orientations of the field.

calculation with $\eta_1=\phi_0(\mathbf{R},\alpha)$. As shown in Fig. 3, a very weak crossover is possible for a small range of parameters, e.g., $3.0 < \eta < 4.2$ for $\bar{\mu}=0$. This is so small that its weak crossover may be an artifact of the variational calculation. We find that the inclusion of a paramagnetic term further reduces its anisotropy. Any anisotropy that

would exist in the absence of the paramagnetic coupling is reduced because the paramagnetic limit has a greater effect for the direction in which the upper critical field is larger. Similar results are obtained for other even-parity representations.⁶

IV. IMPURITY SCATTERING

We consider the E_{1u} representation to illustrate the effect of impurity scattering on the upper critical field. We assume nonmagnetic and s -wave impurity scattering. The upper critical field can be computed by solving the gap equation, Eq. (7), with the self-consistent equation for impurity self-energy. For the E_{1u} state, these equations can be diagonalized *exactly* even in the presence of impurity scattering. When $\mathbf{H}||\hat{z}$ the upper critical field occurs for

$$\Delta(\mathbf{k}_f, \mathbf{R}) = \hat{z} [a\phi_2(\mathbf{R})\psi^*(\mathbf{k}_f) + b\phi_0(\mathbf{R})\psi(\mathbf{k}_f)], \quad (31)$$

where again $\psi(\mathbf{k}_f) \sim k_x + ik_y$. This differs from the order parameter of the clean limit, Eq. (24), by a different combination of ϕ_0 and ϕ_2 terms. The impurity self-energy has the following forms:

$$\langle f(\mathbf{k}_f, \mathbf{R}, \epsilon) \rangle_{\mathbf{k}_f} = \hat{z} d(\epsilon) \phi_1(\mathbf{R}), \quad (32)$$

$$\langle f(\mathbf{k}_f, \mathbf{R}, \epsilon) \rangle_{\mathbf{k}_f} = -ie(\epsilon) \phi_1(\mathbf{R}). \quad (33)$$

It can be shown that $d(\epsilon)$ and $e(\epsilon)$ are a real-valued odd and even function of ϵ , respectively.

By putting Eqs. (31)–(33) into Eqs. (7)–(9) and using the formula (23), we obtain a set of coupled equations for a , b , d , and e :

$$\frac{a}{\lambda} = 4\pi T \sum_{\epsilon \geq 0} \int_0^\infty d\tau \left\langle \exp \left[-2\tau(\epsilon + \pi w_0) - \frac{p^2}{2} \right] \left[\cos(2\tau\mu H) \left\{ a \left[1 - 2p^2 + \frac{p^4}{2} \right] + b \frac{p^2}{\sqrt{2}} \right\} |\psi|^2 + w_0 \left[\sqrt{2}p - \frac{p^3}{\sqrt{2}} \right] |\psi| \text{Re} \{ I(\epsilon) \exp(2i\tau\mu H) \} \right] \right\rangle, \quad (34)$$

$$\frac{b}{\lambda} = 4\pi T \sum_{\epsilon \geq 0} \int_0^\infty d\tau \left\langle \exp \left[-2\tau(\epsilon + \pi w_0) - \frac{p^2}{2} \right] \left[\cos(2\tau\mu H) \left\{ a \frac{p^2}{\sqrt{2}} + b \right\} |\psi|^2 - w_0 p |\psi| \text{Re} \{ I(\epsilon) \exp(2i\tau\mu H) \} \right] \right\rangle, \quad (35)$$

where $\text{Re} \{ \}$ denotes a real part of the argument and $I(\epsilon) = d(\epsilon) + ie(\epsilon)$. The equation for $I(\epsilon)$ becomes

$$I = 2\pi \int_0^\infty d\tau \left\langle \exp \left[-2\tau(\epsilon + \pi w_0) + 2i\tau\mu H - \frac{p^2}{2} \right] \left[\left\{ a \left[-\sqrt{2}p + \frac{p^3}{\sqrt{2}} \right] + bp \right\} |\psi| + w_0(1-p^2)I \right] \right\rangle. \quad (36)$$

The upper critical field is the largest eigenvalue of H in Eqs. (34)–(36). The results are summarized in Fig. 4. Note that the impurity scattering reduces the values of H_{c2} from the clean limit at all temperatures. Paramagnetic coupling limits the upper critical fields away from T_c and reduces the range of the Ginzburg-Landau region where H_{c2} depends linearly on temperature. Close to T_c

we obtain

$$\frac{h_{c2}^{\parallel}}{t_c^2} = \frac{5(3+\sqrt{6})}{21\zeta(3)} \left[1 + \frac{31\pi^4}{1008\zeta(3)} \frac{\bar{w}_0}{t_c} \right] \left[1 - \frac{t}{t_c} \right], \quad \bar{w}_0 \ll 1. \quad (37)$$

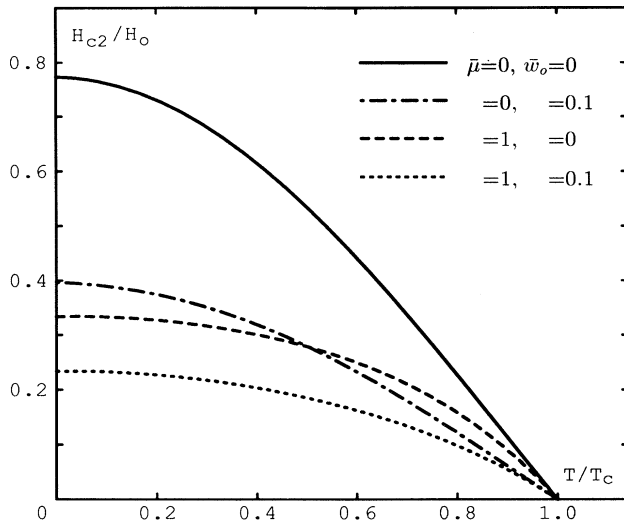


FIG. 4. Plot of H_{c2}^{\parallel}/H_0 vs T/T_c for the E_{1u} representation when $\mathbf{H} \parallel \hat{c}$. Note that T_c is a transition temperature in the presence of impurity scattering and the vertical axis is scaled by the same unit H_0 as in the pure case. Impurity scattering reduces the value of H_{c2} for all temperature. The paramagnetic effect reduces the range of the linear T dependence of H_{c2} close to T_c .

For $\mathbf{H} \parallel \hat{x}$ the upper critical field is independent of the paramagnetism and the impurity self-energy terms vanish, $\langle \mathbf{f} \rangle = \langle f \rangle = 0$. The upper critical field is then computed by a simple substitution of $\epsilon \rightarrow \epsilon + \pi w_0$ in the gap equation of the pure case, Eq. (12). Close to T_c we derive a general expression:

$$\frac{dh_{c2}}{dt} = t_c \frac{S(0)}{S(\bar{w}_0/t_c)} \left[\frac{dh_{c2}^1}{dt} \right]_{\text{pure}}, \quad (38)$$

where

$$S(x) = \sum_{n \geq 0} (2n + 1 + x)^{-3}. \quad (39)$$

Note that Eq. (38) is valid for any cases in which $\langle \mathbf{f} \rangle = \langle f \rangle = 0$. This includes the nonidentity representations of even-parity states such that $\langle \Delta(\mathbf{k}_f) \rangle = 0$. In the plot of H_{c2}/H_0 vs T/T_c , the slope of H_{c2} at T_c is generally smaller than that of pure superconductor due to a large reduction of T_c by impurity scattering.⁵ On the

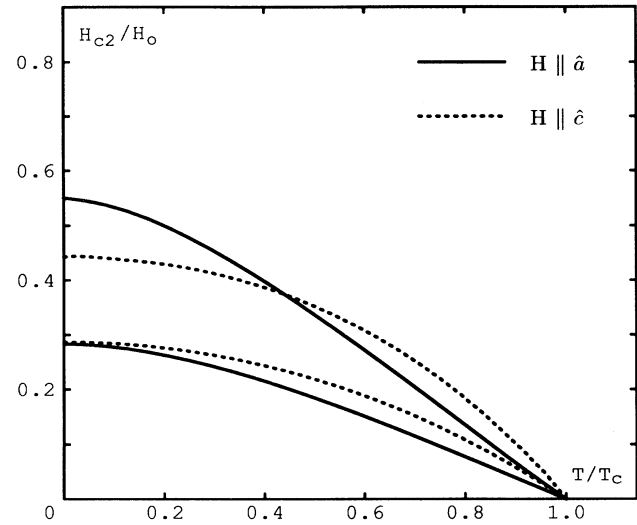


FIG. 5. Plot of H_{c2}^{\parallel} and H_{c2}^{\perp} vs T for the E_{1u} representation. We choose $\eta=3.37$ and $\bar{\mu}=0.68$ as in Fig. 1. The top two curves are in the clean limit, while the bottom two are for $\bar{w}_0=0.1$. Note that impurity scattering can move the crossover point to lower temperature.

contrary the impurity scattering can enhance the values of H_{c2} for the identity representation in which there is no reduction of T_c .¹⁶ In Fig. 5 we show the effect of impurity scattering on the anisotropy of H_{c2} . The values of H_{c2} are reduced by impurity scattering for both directions, while the crossover point moves towards lower temperature. This might explain the fact that some experiments for UPt_3 do not show a distinct crossover at finite temperature.^{2,3}

ACKNOWLEDGMENTS

This work was done in part during C.H.C.'s stay at the Center for Theoretical Physics (SNU, Korea), and also at the University of Bayreuth. He thanks D. Rainer for many useful discussions, and the Alexander von Humboldt Foundation for financial support. The work of J.A.S. was supported by the NSF (Grant No. DMR 91-20521) through the Materials Research Center at Northwestern University.

¹U. Rauchschwalbe, *Physica B* **147**, 1 (1987).

²J. W. Chen, S. E. Lambert, M. B. Maple, J. L. Smith, G. R. Stewart, and J. O. Willis, *Phys. Rev. B* **30**, 1583 (1984).

³U. Rauchschwalbe, U. Ahlheim, F. Steglich, D. Rainer, and J. M. Franse, *Z. Phys. B* **60**, 379 (1985).

⁴B. S. Shivaram, T. F. Rosenbaum, and D. G. Hinks, *Phys. Rev. Lett.* **57**, 1259 (1986).

⁵E. A. Knetsch, J. A. Mydosh, R. H. Heffner, and J. L. Smith, *Physica B* **165-166**, 373 (1990).

⁶C. H. Choi and J. A. Sauls, *Phys. Rev. Lett.* **66**, 484 (1991).

⁷G. E. Volovik and L. P. Gorkov, *Zh. Eksp. Teor. Fiz.* **88**, 1412 (1985) [*Sov. Phys. JETP* **61**, 843 (1985)].

⁸F. Steglich *et al.*, *Physica C* **185-189**, 379 (1991).

⁹I. A. Luk'yanchuk and V. P. Mineev, *Zh. Eksp. Teor. Fiz.* **93**, 2045 (1987) [*Sov. Phys. JETP* **66**, 1168 (1987)].

¹⁰C. H. Choi and P. Muzikar, *Phys. Rev. B* **39**, 9664 (1989).

¹¹J. A. X. Alexander, T. P. Orlando, D. Rainer, and P. M. Tedrow, *Phys. Rev. B* **31**, 5811 (1985).

¹²A. A. Abrikosov, L. P. Gorkov, and I. E. Dzyaloshinski, *Methods of Quantum Field Theory in Statistical Physics* (Dover, New York, 1975), p. 331.

¹³A numerical calculation shows that anisotropy of the magnetic susceptibility does not lead to a large change in the anisotropy of H_{c2} . For example, an anisotropy of 50% in the sus-

ceptibility, $\chi_{\parallel}/\chi_{\perp}=0.5$, yields less than a 10% change of $H_{c2}^{\perp}/H_{c2}^{\parallel}$ for the s -wave superconductor at $T=0$.

¹⁴E. Helfand and N. R. Werthamer, Phys. Rev. **147**, 288 (1966).

¹⁵M. Zhitomirskii, Pis'ma Zh. Eksp. Teor. Fiz. **49**, 333 (1989)

[Sov. Phys. JETP Lett. **49**, 379 (1989)].

¹⁶N. R. Werthamer, E. Helfand, and P. C. Hohenberg, Phys. Rev. **147**, 295 (1966).